Questioning the relationship between the $\chi 4$ susceptibility and the dynamical correlation length in a glass former

Rémy Colin, Ahmed M. Alsayed, Cyprien Gay, Bérengère Abou

Questioning the relationship between the χ_4 susceptibility and the dynamical correlation length in a glass former

Rémy Colin [*a], Ahmed M. Alsayed [b], Cyprien Gay [a] and Bérengère Abou [*a]
[a] *Laboratoire Matière et Systèmes Complexes, UMR CNRS 7057 & Université Paris Diderot, 10 rue A. Domon et L. Duquet, 75205 Paris Cedex 13, France.*
E-mail: remy.colin@univ-paris-diderot.fr; berengere.abou@univ-paris-diderot.fr;
[b] *Complex Assemblies of Soft Matter Laboratory, UMI CNRS 3254, Rhodia INC., 350 G. Patterson Blvd, Bristol PA 19007, USA.*
(Dated: March 13, 2015)

Clusters of fast and slow correlated particles, identified as dynamical heterogeneities (DHs), constitute a central aspect of glassy dynamics. A key ingredient of the glass transition scenario is a significant increase of the cluster size ξ_4 as the transition is approached. In need of easy-to-compute tools to measure ξ_4, the dynamical susceptibility χ_4 was introduced recently. Here, we investigate DHs in dense microgel suspensions using image correlation, and compute both χ_4 and the four-point correlation function G_4. The spatial decrease of G_4 provides a direct access to ξ_4, which is found to grow significantly with increasing volume fraction. However, this increase is not captured by χ_4. We show that the assumptions that validate the connection between χ_4 and ξ_4 are not fulfilled in our experiments. Our findings question the relevance of the broadly used χ_4 in describing DHs.

PACS numbers: 05.40.-a, 64.70.pv, 64.70.qd, 66.30.hh

Understanding the glass transition and the out-of-equilibrium glassy dynamics remains a challenge in condensed matter physics. In practice, glass transitions are observed in various systems, such as molecular liquids, colloids or granular materials [1–3]. Among all, dense colloids are model systems with a glass transition at ambient temperature upon increasing volume fraction [4]. They display slow but accessible timescales and can be probed with simple optical techniques such as microscopy and dynamic light scattering [5, 6].

Over the last 15 years, dynamical heterogeneities (DHs) have been recognized as a promising feature in understanding slow relaxation processes in glass-forming systems [7–9]. DHs consist of fast and slow clusters of dynamically correlated particles, coexisting in the material, with the idea that a dynamical correlation length – representing the clusters size – diverges when approaching the glass transition [10–16]. Dynamical heterogeneities are predicted by theories and have been observed in numerical simulations [11, 17–23] and experimental works [24–32]. They can mainly be quantified with tools such as four-point correlation functions G_4, whose spatial dependence gives a direct access to the dynamical correlation length ξ_4, or with a dynamical susceptibility χ_4 which has recently been proposed as an easy-to-compute indirect tool [11, 24].

Here, we investigate DHs with both a four-point correlation function G_4 and its associated dynamical susceptiblity χ_4, in dense suspensions of soft microgel particles, by performing image correlation. With the direct tool G_4, we measure a significant growth of the dynamical correlation length ξ_4 with increasing volume fraction. We then investigate the validity of the dynamical susceptibility χ_4 as a tool to extract the dynamical correlation length ξ_4, and analyze the reason why it fails to quantify the growth of ξ_4.

From a theoretical point of view, let us consider a system described by a local order parameter $q_{\mathbf{j},t}(\tau)$, here defined as the time correlation of the observable quantity (*e.g.* local density, particle position, transmitted light intensity) between time t and $t+\tau$ at point $\mathbf{j}$. A space-averaged and a space-time-averaged order parameters, $Q_t(\tau) = \langle q_{\mathbf{j},t}(\tau)\rangle_{\mathbf{j}}$ and $Q(\tau) = \langle Q_t(\tau)\rangle_t$ respectively, are constructed so that the averaged time-correlation function $Q(\tau)$ measures the relaxation dynamics of the system. This quantity decays from 1 to 0 as particles move a characteristic distance between t and $t+\tau$ [33].

A direct route to the correlation length ξ_4 is the 4-point correlator $G_4^{\mathrm{vect}}(\mathbf{r},\tau)$ which reflects how $q_{\mathbf{j},t}(\tau)$ is correlated between points separated by $\mathbf{r}$:

$$\begin{aligned} G_4^{\mathrm{vect}}(\mathbf{r},\tau) &= \langle (q_{\mathbf{j}+\mathbf{r},t}(\tau) - q_{\mathbf{j}+\mathbf{r}}(\tau))(q_{\mathbf{j},t}(\tau) - q_{\mathbf{j}}(\tau))\rangle_{\mathbf{j},t} \\ &= \langle q_{\mathbf{j}+\mathbf{r},t}(\tau) q_{\mathbf{j},t}(\tau)\rangle_{\mathbf{j},t} - \langle q_{\mathbf{j}+\mathbf{r}}(\tau) q_{\mathbf{j}}(\tau)\rangle_{\mathbf{j}} \end{aligned} \quad (1)$$

where $q_{\mathbf{j}}(\tau) = \langle q_{\mathbf{j},t}(\tau)\rangle_t$. The corresponding 4-point correlation function $G_4(r,\tau)$ is defined as,

$$G_4(r,\tau) = \langle G_4^{\mathrm{vect}}(\mathbf{r},\tau)\rangle_{r<|\mathbf{r}|<r+\delta r}, \quad (2)$$

with δr chosen such that the average runs over a sufficient number of points. In a system with a dominant dynamical correlation length scale $\xi_4(\tau)$, the correlation function decays at large r as:

$$G_4(r,\tau) \sim \frac{1}{r^p}\exp(-r/\xi_4(\tau)) \quad (3)$$

Equation (3) defines the dynamical correlation length ξ_4.

*R.C.'s current address: Max Planck Institute for Terrestrial Microbiology, Karl-von-Frisch Strasse 16, 35043 Marburg, Germany

Another tool was introduced recently to characterize dynamical heterogeneities [18], namely the dynamical susceptibility $\chi_4(\tau)$. It can be measured as the variance of the temporal fluctuations of $Q_t(\tau)$:

$$\chi_4(\tau) = N(\langle Q_t^2(\tau)\rangle_t - \langle Q_t(\tau)\rangle_t^2) \quad (4)$$

with N the number of points in space under consideration. Let us see how χ_4 is indirectly connected to ξ_4. Since $Q_t(\tau) \equiv \langle q_{\mathbf{j},t}(\tau)\rangle_{\mathbf{j}}$, it can be shown that χ_4 is related to G_4 by:

$$\chi_4(\tau) = \sum_{\mathbf{r}} G_4^{\text{vect}}(\mathbf{r},\tau) \quad (5)$$

which can be expressed in the continuous limit as :

$$\chi_4(\tau) = \rho \int \mathrm{d}^2\mathbf{r}\, G_4(|\mathbf{r}|,\tau) \quad (6)$$

with ρ the average density of points in space. It was recently proposed [18] to use $G_4(r,\tau) \sim A(\tau)/r^p \exp(-r/\xi_4(\tau))$ and Eq. (6) to clarify the link between $\chi_4(\tau)$ and $\xi_4(\tau)$. In two dimensions, $\chi_4(\tau)$ is then :

$$\chi_4(\tau) \sim A(\tau)\, 2\pi\rho\, \xi_4^{2-p}(\tau) \quad (7)$$

The peak of $\chi_4(\tau)$ was proposed and used widely in numerical simulations and experiments [24, 25, 27, 34, 35] to determine the time for which the dynamics is the most heterogeneous and indirectly, the correlation length value ξ_4. As stated in [18], the growing peak in χ_4 upon increasing volume fraction reveals the growth of a dynamical correlation length if the assumptions made for the scaling of G_4 are fulfilled.

Our experimental system consists of a suspension of thermosensitive microgels, made of pNIPAm (poly-N-isopropylacrylamide) crosslinked with BIS (N,N'-methylenebisacrylamide), whose synthesis is described in [14]. The microgel diameter decreases with temperature, which provides a unique way of tuning volume fraction with an external parameter [36, 37]. The microgel suspension was investigated at various volume fractions in the *supercooled states*, close to the glass transition. The volume fraction was increased in a quasistatic way, allowing the system to relax between each step and reach an equilibrium state. A weak particle size polydispersity was used to suppress crystallisation occuring at high volume fraction (see sample preparation details below).

A local order parameter, $q_{\mathbf{j},t}$, defined from the normalized frame intensity $i_{\mathbf{j},\mathbf{j}'}$ as,

$$q_{\mathbf{j},t}(\tau) = \langle i_{\mathbf{j},\mathbf{j}'}(t+\tau) i_{\mathbf{j},\mathbf{j}'}(t)\rangle_{\mathbf{j}'\in ROI[\mathbf{j}]}, \quad (8)$$

was measured to perform image correlation analysis (see details below), a suitable technique when particle trajectories cannot be resolved individually. Figure 1-a shows the ensemble-averaged order parameter $Q(\tau) = \langle q_{\mathbf{j},t}(\tau)\rangle_{\mathbf{j},t}$, similar to the one in [25, 38, 39] in the microgel suspension at various volume fractions. It decreases from its maximal value – ideally 1 at $\tau = 0$ – to 0 at the largest lag times, with a typical decay time $\tau^\star$. It is intuitive that $\tau^\star$ is related to the particles dynamics : as the particles get farther from their initial positions with increasing lag time τ, the time correlation function $Q(\tau)$ between two frames separated by τ gets smaller on average. With increasing volume fraction, the relaxation time $\tau^\star$, defined by $Q(\tau^\star) = 0.25$ [49], increases by three orders of magnitude, revealing the suspension dynamics slowing down.

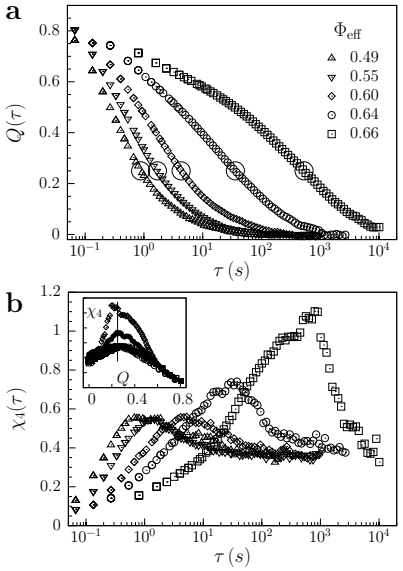

FIG. 1 Mean correlation function $Q(\tau)$ and dynamical susceptibility $\chi_4(\tau)$. They are measured in the microgel suspension with increasing volume fraction between $\Phi_{\text{eff}} = 0.49$ and $\Phi_{\text{eff}} = 0.66$. In (a), the values of the typical decay time $\tau^\star$ of $Q(\tau)$, denoted by large empty circles, are: 0.88, 1.7, 4.3, 36 and $5.3\,10^2$ s. In (b), the peak value of χ_4 increases with volume fraction, suggesting the increase of a spatial correlation length. The inset reveals that the peak value is reached approximately for $Q(\tau) = 0.25$ (vertical line), the value chosen to estimate the typical decay time $\tau^\star$.

The dynamical susceptibility $\chi_4(\tau)$ is shown in Figure 1-b. It exhibits a maximum whose value increases with volume fraction. In the inset, $\chi_4(\tau)$ is plotted as a function of $Q(\tau)$. Its maximum is reached for approximately the same value of $Q(\tau)$, corresponding to the suspension relaxation time $\tau^\star$. Under the assumptions detailed in [18], the increase of the peak value $\chi_4(\tau^\star)$ with volume fraction suggests an increase of the spatial correlation length $\xi_4(\tau^\star)$ with volume fraction, see Eq. (7).

Let us now focus on the direct measurement of dynamical heterogeneities with a normalized 4-point correlation function $G_4(r,\tau)/G_4(0,\tau)$ [11, 19]. Figure 2-a shows $G_4(r,\tau^\star)/G_4(0,\tau^\star)$ measured in the microgel suspension with increasing volume fraction at time $\tau^\star$, consistent with the peak value of χ_4 (see inset of Figure 2-b), where dynamical heterogeneities are expected to be at their maximum. At low volume fraction, $G_4(r,\tau^\star)/G_4(0,\tau^\star)$ exhibits an exponential decay on a length scale a =

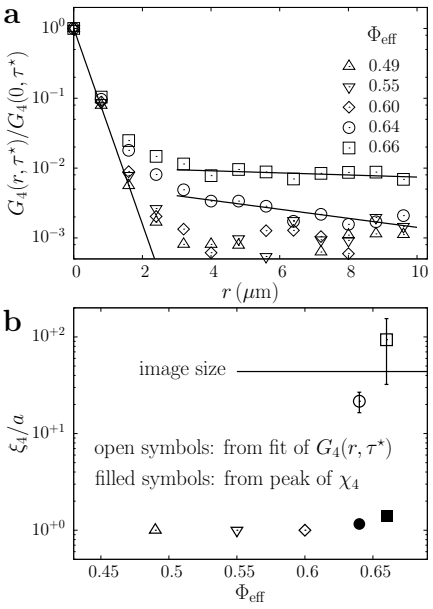

FIG. 2 Normalized 4-point correlation function $G_4(r,\tau^\star)/G_4(0,\tau^\star)$ and correlation length $\xi_4(\tau^\star)$ (inset). (a): At small r, the correlation function exhibits a first exponential decay with a lengthscale $a = 0.31\,\mu$m, which we identify with the microgel radius. It is followed by a second decay at large r which gets slower with increasing volume fraction, indicating that the spatial correlations increase. We define the critical radius r_c as the intersection of both asymptotes. The solid lines correspond to fits according to Eq. (9) with $p = 0$. (b): The correlation length ξ_4 extracted from the fits of G_4 (open symbols) increases significantly with volume fraction. The highest value of ξ_4 is larger than the image size (horizontal line) and must be considered with caution. Values: $\xi_4/a = 93 \pm 63$ at $\Phi_{\mathrm{eff}} = 0.66$; $\xi_4/a = 22 \pm 5$ at $\Phi_{\mathrm{eff}} = 0.64$; At $\Phi_{\mathrm{eff}} = 0.60$, 0.55 and 0.49, the second decay cannot be quantified and we identify the correlation length with the particle radius, $\xi_4 = a$. The values of the correlation length derived from the peak value of χ_4 (filled symbols) are significantly lower.

$0.31\,\mu$m corresponding approximately to the microgel radius, with which it will hereafter be identified [50]. This suggests that $\xi_4 = a$ at low volume fraction. For the two highest volume fractions $\Phi_{\mathrm{eff}} = 0.64$ and $\Phi_{\mathrm{eff}} = 0.66$, the same exponential decay at small r is followed by a second decay at large r. This decay becomes slower with increasing volume fraction, directly suggesting the increase of spatial correlations as the glass transition is approached. The high volume fraction data in Figure 2-a for $G_4(r)$ were fit in the range $r = 3 - 10\,\mu$m, corresponding to the large r-regime, with the following family of functions, following Eq. (3):

$$G_4(\mathrm{r},\tau^\star)/G_4(0,\tau^\star) \propto K_\Phi \left(\frac{a}{r}\right)^p \exp\left(-\frac{r}{\xi_4(\tau^\star)}\right) \qquad (9)$$

where the exponent p, the correlation length ξ_4, and coefficient K_Φ are adjustable parameters [51]. The value $p \sim 0$ was found to provide the best adjustment. The

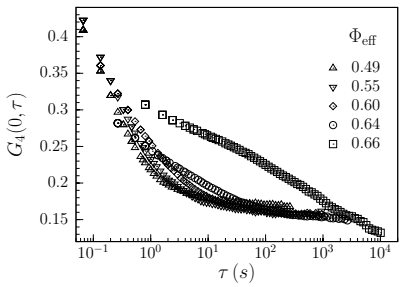

FIG. 3 Prefactor $G_4(0,\tau)$ in the microgel suspension as volume fraction increases. It decreases substantially with the lag time, and is found to slightly depend on volume fraction in the microgel suspension.

correlation length $\xi_4(\tau^\star)$, shown in Figure 2-b and extracted from the fit, increases significantly with volume fraction, and reaches a value (29 ± 19 microns) that exceeds the size of the observed field (13.6×13.6 microns) for the highest volume fraction investigated.

Given our experimental data for G_4, let us investigate how reliably the growth of ξ_4 can be inferred from the growing peak in χ_4. Since χ_4 and G_4 are related through Eq. (6), let us investigate G_4 in more detail. As shown in Fig. 2-a, G_4 displays two spatial regimes for the highest volume fractions, with a crossover radius corresponding to approximately 5 particle radii ($r_c = 1.4\,\mu$m for $\Phi_{\mathrm{eff}} = 0.66$ and $r_c = 1.7\,\mu$m for $\Phi_{\mathrm{eff}} = 0.64$). We now estimate both parts of the integral in Eq. (6), $r < r_c$ and $r > r_c$, as $\int_0^{r_c} 2\pi r \exp(-r/a)\mathrm{d}r$ and $\int_{r_c}^{\infty} 2\pi r K_\Phi \exp(-r/\xi_4)\mathrm{d}r$. The quantity K_Φ was found to depend on volume fraction, as $K_{\Phi=0.66} = 0.0105 \pm 0.0016$ and $K_{\Phi=0.64} = 0.0063 \pm 0.0015$. For $\Phi_{\mathrm{eff}} = 0.66$, we calculate that the $r < r_c$ part of the integral in Eq. (6) contributes about 1% to the entire integral, while for $\Phi_{\mathrm{eff}} = 0.64$, it represents more than 25% of the entire integral. Thus, at $\Phi_{\mathrm{eff}} = 0.64$, the short distance contribution to the integral pollutes the quantity χ_4, devoiding it of any reliable information on collective behaviour. This is even more pronounced at lower volume fractions.

Since the effect of the small scale contribution is 25% at $\Phi_{\mathrm{eff}} = 0.64$ and smaller at $\Phi_{\mathrm{eff}} = 0.66$, let us now assume it can be neglected at first order. Using Eq. (9) with $p = 0$, Eq. (7) writes:

$$2\pi\,\rho\,\xi_4^2(\tau^\star) \sim \frac{\chi_4(\tau^\star)}{K_\Phi\,G_4(0,\tau^\star)} \qquad (10)$$

The quantity $G_4(0,\tau)$, displayed in Figure 3, was found to decrease with the lag time τ and slightly depend on volume fraction. We find that $K_{0.64}\,G_4(0,\tau^\star) = 0.0011$ at $\Phi_{\mathrm{eff}} = 0.64$ and $K_{0.66}\,G_4(0,\tau^\star) = 0.0020$ at $\Phi_{\mathrm{eff}} = 0.66$. Since the prefactor $A(\tau^\star) = K_\Phi\,G_4(0,\tau^\star(\Phi))$ depends on volume fraction, we can not obviously estimate the growth of ξ_4 with volume fraction, using $\chi_4(\tau^\star)$ alone.

Going back to Fig 1, the growth of the correlation length that would be derived from χ_4 if one were to use $2\pi\,\xi_4^2(\tau^\star)A = \chi_4(\tau^\star)$ while ignoring the two sources

of error described above, is estimated. At low volume fraction $\Phi_{\rm eff} = 0.49, 0.55$ and 0.6, the peak value of χ_4 is a constant. Since no correlations are expected, the correlation length is set equal to the particle size, $\xi_4 = a$. This also sets the value of the prefactor A. At higher volume fraction, keeping the same value A for the whole set of data yields $\xi_4^{\Phi_{\rm eff}=0.64} = 1.16a$ and $\xi_4^{\Phi_{\rm eff}=0.66} = 1.41a$. The growth of this estimate of ξ_4 is widely underestimated as compared to the direct measurement (Fig. 2-b).

In conclusion, with the standard direct tool G_4, we measure the growth of a dynamical correlation length ξ_4 from 1 to 93 ± 63 particle radii with increasing volume fraction in our soft microgel suspension. This shows that the dynamics become highly heterogeneous in space when approaching the glass transition, consistent with the broad theoretical picture [40]. Recently, most studies have focused on the dynamical susceptibility χ_4 as a convenient and indirect tool to quantify DHs. However, our results suggest that the risk of error in estimating the dynamic correlation length ξ_4 through χ_4 must be addressed when trying to link the dynamic heterogeneities with other features of the glass transition, such as *e.g.* the local structure [41, 42] or the soft modes of vibration [43, 44]. In other words, χ_4 should *a priori never* be used as a quantitative indicator of the increase of the spatial correlations, before having first performed a direct measurement of G_4 to estimate its validity. This non-universality of χ_4 was recently discussed from a theoretical perspective [45, 46]. However, as it is the variance of the time correlation function $Q_t(\tau)$, the susceptibility χ_4 is expected to remain an indicator of the lag time for which the dynamics is the most heterogeneous. In our experiments, the peak occurs approximately at the suspension relaxation time $\tau^\star$ defined by $Q(\tau^\star) = 0.25$, see Fig. 1. The origin of the failure of χ_4 is related to the fact that *(i)* it contains the correlations at the scale of the particle radius and *(ii)* the prefactor $A(\tau)$ in Eq. (7) varies with volume fraction. This result suggests investigating other glass forming materials and using techniques other than image correlation to understand which physical properties generate this predominance of small distance correlations and impair the relevance of χ_4.

Acknowledgements

We thank E. Bertin, L. Cippeletti, O. Dauchot, J.-B. Fournier, F. van Wijland and L. Wilson for fruitful discussions, and A. Callan-Jones for a critical reading of the manuscript. We acknowledge support from PICS-CNRS *SofTher* (B.A. (P.I.), R.C. and A.A.).

Microgel suspension volume fraction. The microgel suspension is prepared by mixing two suspensions of microgel particles with a diameter ratio 1:1.8, constant over the range of temperature we used. The numerical fraction of large particles is 18%. The smaller particle diameter is $1.03 \pm 0.01\,\mu$m at 20 °C and decreases down to $0.862 \pm 0.006\,\mu$m at 30 °C. An effective volume fraction was assigned to the microgel suspension at T = 30 °C in the following way. Latex probes of radius $R = 0.5\,\mu$m comparable to that of the microgels, were added to the suspension. Their mean-squared displacement (MSD) was measured and found to increase linearly with time, which defines a diffusion coefficient D, $\langle \Delta r^2(\tau) \rangle_{i,t} = 4D\tau$. A suspension viscosity was defined as $\eta = k_B \mathrm{T}/6\pi RD$. The viscosity was between 8 and 74 mPa.s, at T = 30 °C. It was shown that for pNIPAm suspensions similar to ours, $\eta/\eta_{\rm solvent}$ can be used to estimate the volume fraction [47]. In our case, the volume fraction at $T = 30\,^\circ$C was approximately $\Phi_{30} = 0.45$. The volume fraction for all bath temperatures T was derived using the relation $\Phi_{\rm eff}(\mathrm{T}) = (d(\mathrm{T})/d_{30})^3\,\Phi_{30}$, where d is the diameter of the microgels at temperature T, measured with Dynamic Light Scattering experiments, and d_{30} refers to their diameter at T = 30 °C.

Sample preparation and video recording. The microgel suspension was injected in a $3 \times 3\,\mathrm{mm}^2$ chamber made of a microscope plate and a coverslip separated by a $250\,\mu$m thick adhesive spacer. The chamber was sealed with araldite glue to avoid evaporation and contamination. The samples were observed on a inverted Leica DM IRB microscope with a ×100 oil immersion objective. The objective temperature was adjusted with a Bioptechs objective heater within ±0.1 °C. The sample temperature was maintained through the immersion oil in contact. A CCD camera (FOculus 124B), coupled to the microscope, was recording the microgel suspension dynamics. It was running at a frame rate from 30 down to 0.375 fps for a few minutes to several hours, depending on the suspension dynamics. The region of observation was chosen at least $100\,\mu$m away from the sample edges to avoid boundary effects.

Image correlation analysis. Films consist of successive video frames, each described by a matrix of pixels $\mathbf{p}$ of intensity $I_{\mathbf{p}}(t)$, where $\mathbf{p}$ is the two-dimensional index of the pixel position and t the temporal position of the frame in the film. Possible global variations of illumination and contrast along the film are wiped out using the normalized frame intensity $i_{\mathbf{p}}(t)$ at pixel $\mathbf{p}$:

$$i_{\mathbf{p}}(t) = \frac{I_{\mathbf{p}}(t) - \langle I_{\mathbf{p}}(t) \rangle_{\mathbf{p}}}{\sqrt{\langle (\delta I_{\mathbf{p}}(t))^2 \rangle_{\mathbf{p}}}} \qquad (11)$$

with $\delta I_{\mathbf{p}}(t) = I_{\mathbf{p}}(t) - \langle I_{\mathbf{p}}(t) \rangle_{\mathbf{p}}$, and $\langle \cdot \rangle_{\mathbf{p}}$ the average over all the pixels in the frame. Each frame was divided into non-overlapping squared Regions Of Interest, ROI, of dimension equivalent to a particle size. ROI[$\mathbf{j}$] is centered around pixel $\mathbf{j}$. The normalized frame intensity $i_{\mathbf{p}}(t)$ at pixel $\mathbf{p}$ is now denoted as $i_{\mathbf{j},\mathbf{j}'}(t) \equiv i_{\mathbf{p}}(t)$, with $\mathbf{j}$ the center of ROI[$\mathbf{j}$] and $\mathbf{j}' \in$ ROI[$\mathbf{j}$]. For each frame, following [39], the local order parameter, $q_{\mathbf{j},t}(\tau)$, was defined as :

$$q_{\mathbf{j},t}(\tau) = \langle i_{\mathbf{j},\mathbf{j}'}(t+\tau) i_{\mathbf{j},\mathbf{j}'}(t) \rangle_{\mathbf{j}' \in \mathrm{ROI}[\mathbf{j}]}, \qquad (12)$$

Image correlation was performed on regions of dimension 187×187 pixel^2, corresponding to $13.6 \times 13.6\,\mu\mathrm{m}^2$ *i.e.*

and around 200 particles in the field. The dimension of the ROIs sets the spatial resolution. It was chosen as 11px, *i.e.,* equivalent to the particle size. A home-made ImageJ [48] plugin was used to calculate the quantities $Q(\tau)$, $G_4(0,\tau)$, $\chi_4(\tau)$ for each film.

[1] C. Angell, Science **267**, 1924 (1995).

[2] L. Berthier and G. Biroli, Reviews of Modern Physics **83**, 587 (2011), URL http://link.aps.org/doi/10.1103/RevModPhys.83.587.

[3] A. J. Liu and S. R. Nagel, Annual Review of Condensed Matter Physics **1**, 347 (2010), URL http://www.annualreviews.org/doi/abs/10.1146/annurev-conmatphys-070909-104045.

[4] P. N. Pusey and W. van Megen, Nature **320**, 340 (1986).

[5] E. R. Weeks, J. C. Crocker, A. C. Levitt, A. Schofield, and D. A. Weitz, Science **287**, 627 (2000).

[6] W. K. Kegel and A. van Blaaderen, Science **287**, 290 (2000).

[7] M. Ediger, Annual Review of Physical Chemistry **51**, 99 (2000).

[8] R. Richert, Journal of Physics : Condensed Matter **14**, R703 (2002).

[9] H. Sillescu, Journ. of Non-crystalline Solids **243**, 81 (1999).

[10] A. H. Marcus, J. Schofield, and S. Rice, Phys. Rev. E **60**, 5725 (1999).

[11] N. Lacevic, F. W. Starr, T. B. Schrøder, and S. C. Glotzer, Journal of Chemical Physics **119**, 7372 (2003).

[12] P. Wang, C. Song, and H. A. Makse, Nature Physics pp. 526 – 531 (2006).

[13] P. Chaudhuri, W. Kob, and L. Berthier, Phys. Rev. Lett. **99**, 060604 (2007).

[14] R. Colin, A. M. Alsayed, J.-C. Castaing, R. Goyal, L. Hough, and B. Abou, Soft Matter **7**, 4504 (2011), URL http://dx.doi.org/10.1039/C0SM01184C.

[15] G. Biroli and J. P. Bouchaud, in *Structural Glasses and Supercooled Liquids: Theory, Experiment, and Applications*, edited by P. G. Wolynes and V. Lubchenko (John Wiley & Sons, Inc., Hoboken, NJ, USA., 2012).

[16] L. O. Hedges, R. L. Jack, J. P. Garrahan, and D. Chandler, Science **323**, 1309 (2009).

[17] L. Berthier, Phys. Rev. E **69**, 020201 (2004).

[18] L. Berthier, G. Biroli, J.-P. Bouchaud, and R. L. Jack, in *Dynamical Heterogeneities in Glasses, Colloids, and Granular Media*, edited by L. Berthier, G. Biroli, J.-P. Bouchaud, L. Cipelletti, and W. van Saarloos (Oxford University Press, 2011).

[19] C. Dasgupta, A. V. Indrani, S. Ramaswamy, and M. K. Phani, Europhys. Lett. **15**, 307 (1991), ISSN 0295-5075, 1286-4854, URL http://iopscience.iop.org/0295-5075/15/3/013.

[20] C. Donati, S. Franz, S. C. Glotzer, and G. Parisi, Journal of Non-Crystalline Solids **307310**, 215 (2002), ISSN 0022-3093, URL http://www.sciencedirect.com/science/article/pii/S0022309302014618.

[21] M. Vogel and S. C. Glotzer, Phys. Rev. E **70**, 061504 (2004).

[22] D. Chandler, J. P. Garrahan, R. L. Jack, L. Maibaum, and A. C. Pan, Phys. Rev. E **74**, 051501 (2006), URL http://link.aps.org/doi/10.1103/PhysRevE.74.051501.

[23] A. Parsaeian and H. E. Castillo, Phys. Rev. E **78**, 060105 (2008), URL http://link.aps.org/doi/10.1103/PhysRevE.78.060105.

[24] L. Berthier, G. Biroli, J.-P. Bouchaud, L. Cipelletti, D. E. Masri, D. L'Hote, F. Ladieu, and M. Pierno, Science **310**, 1797 (2005), http://www.sciencemag.org/cgi/reprint/310/5755/1797.pdf, URL http://www.sciencemag.org/cgi/content/abstract/310/5755/1797.

[25] K. N. Nordstrom, J. P. Gollub, and D. J. Durian, Phys. Rev. E **84**, 021403 (2011), URL http://link.aps.org/doi/10.1103/PhysRevE.84.021403.

[26] P. Ballesta, A. Duri, and L. Cipelletti, Nature Phys. **4**, 550 (2008).

[27] A. R. Abate and D. J. Durian, Phys. Rev. E **76**, 021306 (2007), URL http://link.aps.org/doi/10.1103/PhysRevE.76.021306.

[28] A. Duri and L. Cipelletti, Europhys. Lett. **76**, 972 (2006).

[29] D. Sessoms, I. Bischofberger, L. Cipelletti, and V. Trappe, Phil. Trans. R. Soc. A **367**, 5013 (2009).

[30] E. R. Weeks, J. C. Crocker, and D. A. Weitz, Journal of Physics : Condensed Matter **19**, 205131 (2007).

[31] T. Narumi, S. V. Franklin, K. W. Desmond, M. Tokuyama, and E. R. Weeks, Soft Matter **7**, 1472 (2011), ISSN 1744-683X, 1744-6848, URL http://pubs.rsc.org/en/Content/ArticleLanding/2011/SM/c0sm00756k.

[32] F. Lechenault, O. Dauchot, G. Biroli, and J. Bouchaud, Europhys. Lett. **83**, 46002 (2008).

[33] O. Dauchot, D. Durian, and M. van Hecke, in *Dynamical Heterogeneities in Glasses, Colloids, and Granular Media*, edited by L. Berthier, G. Biroli, J.-P. Bouchaud, L. Cipelletti, and W. van Saarloos (Oxford University Press, 2011).

[34] C. Crauste-Thibierge, C. Brun, F. Ladieu, D. LHôte, G. Biroli, and J.-P. Bouchaud, Phys. Rev. Lett. **104**, 165703 (2010), URL http://link.aps.org/doi/10.1103/PhysRevLett.104.165703.

[35] D. El Masri, L. Berthier, and L. Cipelletti, Phys. Rev. E **82**, 031503 (2010).

[36] B. R. Saunders and B. Vincent, Advances in Colloid and Interface Science **80**, 1 (1999).

[37] A. Fernandez-Nieves, H. M. Wyss, J. Mattsson, and D. A. Weitz, eds., *Microgel Suspensions: Fundamentals and Applications* (2011), ISBN 9783527321582, 9783527632992, URL http://onlinelibrary.wiley.com/book/10.1002/9783527632992.

[38] L. Cipelletti, H. Bissig, V. Trappe, P. Ballesta, and S. Mazoyer, Journal of Physics: Condensed Matter **15**, S257 (2003), URL http://stacks.iop.org/0953-8984/15/i=1/a=334.

[39] A. Duri, D. A. Sessoms, V. Trappe, and L. Cipelletti, Phys. Rev. Lett. **102**, 085702 (2009), URL http://link.aps.org/doi/10.1103/PhysRevLett.102.085702.

[40] L. Berthier, G. Biroli, J.-P. Bouchaud, and R. L. Jack, *Dynamical Heterogeneities in Glasses, Colloids, and*

Granular Media (Oxford University Press, 2011).
[41] C. P. Royal and S. R. Williams, Physics Report **560**, 1 (2015).
[42] S. Karmakar, C. Dasgupta, and S. Sastry, Annu. Rev. Cond. Matt. Phys. **5**, 255 (2014).
[43] K. Chen, M. L. Manning, P. J. Yunker, W. G. Ellenbroek, Z. Zhang, A. J. Liu, and Y. A. G., Phys. Rev. Lett. **107**, 108301 (2011).
[44] A. Widmer-Cooper, H. Perry, P. Harrowell, and D. R. Reichman, Nature Physics **4**, 711 (2008), ISSN 1745-2473, URL `http://www.nature.com/nphys/journal/v4/n9/full/nphys1025.html`.
[45] R. Pastore, M. Pica Ciamarra, A. de Candia, and A. Coniglio, Phys. Rev. Lett. **107**, 065703 (2011).
[46] O. Takeshi, S. Goto, T. Matsumoto, A. Nakahara, and M. Otsuki, Phys. Rev. E **88**, 062108 (2013).
[47] H. Senff and W. Richtering, The Journal of Chemical Physics **111**, 1705 (1999), URL `http://link.aip.org/link/?JCP/111/1705/1`.
[48] W. S. Rasband, *ImageJ, U. S. National Institutes of Health, Bethesda, Maryland, USA, http://imagej.nih.gov/ij/* (1997-2011).
[49] The decay time $\tau^\star$ can be arbitrarily defined as $Q(\tau^\star) = 0.25$. In the range $0.2 < Q(\tau) < 0.4$, the curves of Q are parallel to each other and the increase in $\tau^\star$ with volume fraction does not depend much on the value of Q.
[50] The microgel radius, measured with Dynamic light scattering experiments, depends on temperature. It is $0.43\,\mu$m at $T = 30\,^\circ$C.
[51] To perform the fits, the weight for each $G_4(r, \tau^\star)$ data point was chosen as the number of pairs of ROIs involved in the average over the whole sample (17×17 ROIs) in Eq. (1) and in the average over an annular region in Eq. (2).